Journal of Nuclear Medicine, published on July 14, 2016 as doi:10.2967/jnumed.116.174433

# The predictive value of early assessment after one cycle of induction chemotherapy with $^{18}$F-FDG-PET/CT and DW-MRI for response to radical chemoradiotherapy in head and neck squamous cell carcinoma

**Authors:**

Kee H Wong[1,2], Rafal Panek[1,2], Liam Welsh[1], Dualta Mcquaid[1], Alex Dunlop[1], Angela Riddell[1], Iain Murray[1,2], Yong Du[1], Sue Chua[1], Dow-Mu Koh[1,2], Shreerang Bhide[1,2], Chris Nutting[1], Wim JG Oyen[1,2], Kevin Harrington[1,2], Kate L Newbold[1].

[1] The Royal Marsden NHS Foundation Trust, Sutton and London, UK

[2] The Institute of Cancer Research, Sutton and London, UK

**First & corresponding author:**

Kee H Wong

Clinical research fellow

The Royal Marsden Hospital

Downs Road

Sutton SM2 5PT

Contact: 02086613638

**Short title:** FMI during induction chemotherapy

**Word Count:** 5150 words

## ABSTRACT

**Objectives:** To assess the predictive value of early assessment (after one cycle of induction chemotherapy (IC)) with $^{18}$F-FDG-PET/CT and DW-MRI for subsequent response to radical chemoradiotherapy in locally advanced head and neck squamous cell carcinoma (HNSCC). **Methods:** 20 patients with stage III-IVa HNSCC prospectively underwent $^{18}$F-FDG-PET/CT and diffusion-weighted MRI (DW-MRI) before and 2 weeks following each cycle of IC (1$^{st}$ cycle - IC1, 2$^{nd}$ cycle - IC2). Response was assessed 3 months after completion of chemoradiotherapy with clinical examination, MRI and $^{18}$F-FDG-PET/CT. Patients with persistent disease were classed as non-responders. Changes in functional and molecular imaging (FMI) parameters following IC1 were compared between responders and non-responders with Mann-Whitney U test. The significance threshold was set at $P<0.05$. **Results:** Responders showed a significantly greater reduction in metabolic tumour volume (MTV)($p=0.03$) and total lesion glycolysis (TLG)($p=0.04$) following IC1 than non-responders. Responders also showed a tendency towards a larger, but statistically non-significant increase in apparent diffusion coefficient following IC1. There was no significant difference in the changes from baseline between the IC1 and IC2 for all FMI parameters indicating that most biological response to IC measured by $^{18}$F-FDG-PET/CT and DW-MRI was observed early after the first cycle of IC. **Conclusion:** Our preliminary data indicate that the $^{18}$F-FDG-PET/CT-derived MTV or TLG, acquired after IC1 are early predictive biomarkers for ultimate response to subsequent chemoradiotherapy. This enables identification of patients at risk of treatment failure at an early time-point, permitting treatment individualisation and consideration of alternative strategies such as radiotherapy dose-escalation or surgery.

**Key words:** Diffusion-weighted MRI, $^{18}$F-FDG-PET/CT, Induction chemotherapy, head and neck squamous cell carcinoma

## INTRODUCTION

Induction chemotherapy (IC) remains a contentious aspect of management for locally advanced head and neck squamous cell carcinoma (HNSCC). To date, four phase III randomised controlled trials have investigated the role of IC prior to chemoradiotherapy for locally advanced HNSCC. Only one study showed an overall survival benefit (*1*). Nevertheless, it is noteworthy that the negative studies had limitations with poor accrual, inadequate power and low radiotherapy completion rates (*2-4*).

Despite contradictory evidence regarding its overall survival benefit, IC remains a standard-of-care in organ sparing approaches in laryngeal cancer and appears to reduce distant failure rates in HNSCC (*5,6*). Good response to IC has been reported to be predictive of complete response to subsequent radiotherapy and long-term disease control (*7,8*). This concept has led to randomised clinical trials such as *ECOG-1308* and *Quarterback*, which are investigating radiotherapy dose reduction in human papillomavirus (HPV)-driven stage III-IV oropharyngeal cancer using complete response to IC as a selection criterion (*9*). Conversely, patients with poor response to IC are at a higher risk of radiotherapy failure and require treatment intensification. Despite being an attractive strategy, IC is associated with increased rates of complications (*10*). Therefore, an early predictive biomarker is essential to identify those who will or will not benefit.

Functional and molecular imaging (FMI) characterise the tumour phenotype by providing quantitiative information on biological processes such as metabolic activity, vascularity and cellularity (*11*). Biological changes measured by FMI are usually evident before morphological changes (*12*) and this confers a potential advantage over conventional imaging for early response assessment. Several studies have identified

$^{18}$F-FDG-PET/CT and diffusion-weighted MRI (DW-MRI) as promising imaging biomarkers for HNSCC (*13-16*), with different, but complementary, biological information from each modality (*17*). The majority of FMI studies are largely based on post-IC imaging but an earlier time-point for assessment during IC is required to allow time for an individualized treatment plan based on tumour response to therapy.

To address these issues, we established a prospective multimodality longitudinal FMI study (INSIGHT) in locally advanced HNSCC scheduled for radical chemoradiotherapy (*18*). Here, we report the results of serial $^{18}$F-FDG-PET/CT and DW-MRI following each cycle of IC in the first 20 patients (target accrual 66). The purpose of this planned interim analysis is three-fold: (a) to assess the appropriateness of early assessment after one cycle of IC with $^{18}$F-FDG-PET/CT and DW-MRI by comparing the difference in changes of FMI parameters between the 1$^{st}$ and 2$^{nd}$ cycle; (b) to identify FMI parameters predictive of ultimate response to subsequent radical chemoradiotherapy and (c) to identify a biological target volume (BTV) in the event of persistent disease.

## MATERIALS AND METHODS

### Study Design

Patients were recruited at The Royal Marsden Hospital between July 2013 and February 2015. Patients with previously untreated histologically proven HNSCC (stage III-IVb) and WHO performance status 0-2 planned for radical chemoradiotherapy, with or without IC, were eligible for the study. This study received approvals from the institutional review board (CCR3926) and research ethical committee (13/LO/0067). All patients provided written consent.

Our standard regimen of IC is 2 cycles of 3 weekly TPF (Docetaxel (75 mg/m$^2$) day 1/Cisplatin (75 mg/m$^2$) day 1/5-fluorouracil (1000 mg/m$^2$) days 1-4). Modifications were permissible for individual patient factors e.g. tinnitus, renal impairment and peripheral neuropathy. Patients prospectively underwent $^{18}$F-FDG-PET/CT and DW-MRI at baseline and 2 weeks following each cycle of IC (1st cycle - IC1, 2nd cycle - IC2). Three weeks following IC, patients proceeded to 6 weeks of radical radiotherapy with concomitant chemotherapy (Cisplatin (100 mg/m$^2$) or Carboplatin (AUC5) days 1 and 29). Macroscopic and microscopic disease (defined on pre-chemotherapy imaging) received 65 Gy and 54 Gy in 30 fractions, respectively, using intensity-modulated radiotherapy with a simultaneous integrated boost. Response was assessed at 3 months following completion of chemoradiotherapy with MRI, $^{18}$F-FDG-PET/CT and clinical examination including nasendoscopy. Patients with evidence of persistent disease at 3 months were classed as non-responders.

**PET/CT Image Acquisition**

PET/CT studies were acquired using Phillips Gemini (London) and Siemens mCT (Sutton) PET/CT scanners. Patients were fasted for 6 hours before the study. 18F-FDG (400 MBq) was injected intravenously if the blood sugar level was <10 mmol/L. Prior to PET acquisition, patients rested for 60 minutes. Patients were positioned on a flat-top couch in their radiotherapy treatment position, using a headrest and 5-point thermoplastic shell. Emission data were acquired from the base of skull to carina (3 min/bed; average 2 bed acquisition). Unenhanced, low dose CT was performed from the base of skull to carina for purposes of attenuation correction and image fusion for anatomical localisation (approximate mAs 50/slice).

**MRI Image Acquisition**

All MRI scans were acquired on a 1.5T scanner (MAGNETOM Aera, Siemens Healthcare, Erlangen, Germany). Patients were set-up on a flat-top MRI couch in the radiotherapy treatment position, using a headrest and 5-point thermoplastic shell. A large flex and spine coils were used. For all images, 200x200 mm field of view (FOV), 2 mm isotropic voxel size and 80 mm cranio-caudal coverage was used. Anatomical $T_2$-weighted (matrix 192, TE/TR: 82/11000 ms) and $T_1$-weighted (matrix 192, TE/TR: 13/794 ms) were acquired first to aid functional MRI planning. DW-MRI sequences (SE-EPI DWI, matrix 96, TE/TR: 61/13400, b values: 50,400,800 s/mm$^2$, NSA=5, FOV 199x199, BW=1000 Hz) were then acquired.

**Image Analysis**

All PET and MRI data were analyzed using RayStation (version 4.6.1, RaySearch Medical Laboratories, AB Stockholm, Sweden), a radiotherapy treatment planning system. RayStation (internally validated for data accuracy) was chosen for its ability to handle large longitudinal multimodality image sets and incorporate radiotherapy dosimetry. Regions of interest (ROIs) encompassing the primary tumor (PT) or involved lymph nodes (LNs) were delineated on each imaging modality by a radiation oncologist. These contours were verified by experienced consultants in nuclear medicine (WO) and radiology (AR).

PET images reconstructed using ordered subset expectation maximisation were used for analysis. Two methodologies were used to generate the metabolic tumour volume (MTV): relative threshold of 40% of maximum standardised uptake volume (SUVmax) ($MTV_{40\%}$) and fixed threshold of SUV3.5 ($MTV_{3.5}$). The baseline value served as the threshold for MTV on subsequent scans. Other PET parameters including

SUVmax and total lesion glycolysis (TLG = SUVmean x MTV) (*19*), were recorded for all ROIs at each time-point.

Anatomical contours for MRI were delineated on $T_2$-weighted images with reference to $T_1$-weighted images. For DW analysis, ROIs were defined on the $T_2$-weighted low b-value images (b50) with reference to the co-registered anatomical contours, excluding regions of necrosis and cysts (Fig. 1). This accounts for potential local deformation of DW images in the vicinity of air-tissue interfaces and dental objects. All b values were used to calculate the apparent diffusion coefficient (ADC). Due to the skewed distribution of ADC values, the median value was chosen as the statistical representation for individual ROI. ADC was recorded separately for PT and LNs.

The radiotherapy planning CT and dosimetry were imported to enable dosimetric analysis. Good co-registrations between FMI images and planning CT were achieved due to immobilisation, allowing rigid transformation of contours across all images.

**Statistical Analysis**

The data were analysed using SPSS statistical software (Version 21.0; IBM Corp, Armonk, NY). Depending on the normality of the data distribution (using Kolmogorov-Smirnov test), the changes in PET and DW-MRI parameters from baseline were compared between IC1 and IC2 using paired t-test (normal) or Wilcoxon signed-rank test (non-normal). Changes in FMI parameters changes following IC1 were compared between responders and non-responders using the Mann-Whitney U test. The significance threshold was set at $p<0.05$. Receiver operator characteristics (ROC) analysis was used to identify and determine the optimal threshold values for parameters with predictive value.

## RESULTS

**Clinical Characteristics**

Patient and treatment characteristics are shown in Table 1. Seventeen out of 20 patients underwent 2 cycles of IC; three patients stopped IC after 1 cycle due to poor tolerance. One patient did not receive concomitant chemotherapy due to persistent myelosuppression following IC. All patients completed chemoradiotherapy within 42 days. Median follow-up was 14 (range 7-25) months.

**Treatment Outcome**

There were 15 responders and 5 non-responders. One responder underwent a modified radical neck dissection due to equivocal radiological appearance post-chemoradiotherapy, but no viable residual disease was found. At the time of analysis, all responders remained alive and disease-free. All five non-responders had locoregional failure: two also developed distant metastases. Only one patient was deemed suitable for salvage surgery and underwent radical pharyngolaryngectomy. He remains disease-free to date. The remaining four non-responders had died by the time of analysis (5-9 months post-chemoradiotherapy).

**FMI - Responders Versus Non-responders**

Baseline $MTV_{40\%}$, $MTV_{3.5}$, $TLG_{40\%}$ and $TLG_{3.5}$ differed significantly between the two groups, but not for SUVmax and SUVmean (Table 2). Responders also showed a significantly greater mean reduction in $MTV_{3.5}$, $TLG_{3.5}$ and $TLG_{40\%}$ post-IC1 than non-responders. The reductions in SUVmax and SUVmean were not discriminative between the two groups post-IC1 but did reach statistical significance post-IC2 ($p=0.01$ and 0.037, respectively). There was a clear association between MTV or TLG response and HPV status (Fig. 2).

There was no significant difference in pre-treatment ADC for both PT and LNs between the two groups (Table 2). For patients with discernible tumour following IC1, the mean ADC for PT was higher in responders than non-responders but this did not reach statistical significance (p=0.089). LNs in responders also showed a greater, but statistically non-significant, increase in ADC post-IC1 than non-responders. The changes in ADC post-IC2 remained non-discriminative between responders and non-responders for both PT (p=0.343) and LNs (p=0.658). The pre-treatment mean ADC was significantly lower in the LNs for HPV-positive in comparison to HPV-negative HNSCC (0.95±0.13 vs. 1.07±0.15 $x10^{-3}$ $mm^2/s$, p=0.025), but no difference was observed in the PT (1.15±0.18 vs. 1.16±0.14 $x10^{-3}$ $mm^2/s$, p=0.93). Cumulatively, a tendency towards a larger increase in ADC post-IC1 was observed in HPV-positive tumours (Fig. 2).

T stage (T1-2 vs. T3-4), N stage (N0-1 vs. N2-3) and tumour grade (G1-2 vs. G3) were all non-predictive of response to chemoradiotherapy (p>0.05). ROC analyses identified $TLG_{40\%}$ as the optimal predictive parameter for treatment response using relative threshold and $MTV_{3.5}$ using fixed threshold. A combination of pre-treatment $TLG_{40\%}$ <300 g and $TLG_{40\%}$ reduction >60% post-IC1 gave an improved sensitivity and specificity of 93% and 80% in predicting complete remission in comparison to individual parameters (Fig. 3). A combination of $MTV_{3.5}$ <50 $cm^3$ and $MTV_{3.5}$ reduction >55% post-IC1 yielded similar result.

**Longitudinal FMI Parameters**

The longitudinal changes in $^{18}$F-FDG-PET/CT and DW-MRI parameters during IC are summarised in Table 3. In 17 evaluable patients, there was no significant difference in the changes from baseline between IC1 and IC2 for all PET parameters. This indicates that most metabolic response or non-response to IC was evident soon after

IC1, with no significant change following a subsequent cycle. This remains the case after dichotomising the data to PT and LNs (Supplemental Table 1). However, it is noteworthy that the differences in SUVmax and SUVmean approached statistical significance (p=0.065 and 0.071, respectively).

Similarly, there was no significant difference in the magnitude of ADC changes between IC1 and IC2. Overall, the dominant trend of ADC observed for both PT and LNs was an increase. As anticipated, there was a significant difference in the anatomical changes for both PT and LNs between IC1 and IC2, with notable additional change after IC2, reaffirming that morphological change in HNSCC following IC lags behind biological change.

**Radiotherapy Dosimetry**

Review of the radiotherapy dosimetry in the non-responders (in relation to the site of persistent disease identified on imaging post-chemoradiotherapy) revealed one marginal and four in-field failures. The patient with marginal failure exhibited an unusual pattern of disease spread with the persistent tumour extending beyond clinical target volume (1 cm isotropic expansion of pre-chemotherapy gross tumour volume). There was significant overlap between persistent disease and MTV post-IC1. For the in-field failures, there was an average volume overlap of 73% with the non-overlapping volume corresponding to areas of progression. This indicates that residual MTV post-IC1 represents a more ‘resistant’ tumour subregion and is, therefore, a potential BTV for radiotherapy dose escalation. A representative case is shown in Fig. 4.

## DISCUSSION

We evaluated early assessment after IC1 using $^{18}$F-FDG-PET/CT and DW-MRI to predict response to subsequent chemoradiotherapy in locally advanced HNSCC. There are three main findings: first, the changes in FMI parameters measured by both modalities after IC1 are representative of its 'full' effect with few additional changes with IC2. This indicates that response assessment using $^{18}$F-FDG-PET/CT and DWI-MRI at this early time-point is clinically relevant. To the best of our knowledge, this is the first study in HNSCC to provide full longitudinal $^{18}$F-FDG-PET/CT and DW-MRI data following each cycle of IC.

Second, $^{18}$F-FDG-PET/CT-derived MTV or TLG, acquired before and after IC1 are early predictors of response to subsequent chemoradiotherapy. The high predictive power achieved by a combination of these parameters enables early stratification of patients into distinct groups based on response and associated risk of subsequent chemoradiotherapy failure. This has important clinical applicability for guiding treatment personalisation. Patients with favorable metabolic response post-IC1 (reduction in MTV >55% or TLG >60%) could be considered for radiotherapy dose reduction, especially HPV-positive patients. On the contrary, those with unfavorable response should be considered for non-standard-chemoradiotherapy approach e.g. radiotherapy dose escalation, addition of novel targeted agents or surgery. IC should also be discontinued immediately in those with metabolic progression (increase in MTV or TLG). These preliminary findings provide the basis for a future interventional study using FMI parameters to stratify patients (Fig. 5).

Third, residual MTV post-IC1 is a potential BTV for radiotherapy dose escalation. This is particularly relevant for those who had suboptimal metabolic response, where

dose escalation to a subvolume of more 'resistant' tumour should be feasible within acceptable tolerance of organs at risk. This may improve the rate of complete remission post-chemoradiotherapy and avert the need for salvage surgery. Conveniently, early assessment after IC1 also allows for a fluent radiotherapy planning workflow without delay if a patient requires dose modification.

Our findings add to a growing body of evidence that pre-treatment MTV and TLG are independent factors associated with local control and survival outcome (*20*), and further highlight their utilities early during IC to guide treatment individualization. Three studies have evaluated response assessment with $^{18}$F-FDG-PET/CT after IC1 in HNSCC (*21-23*). However, none were designed to inform how best to personalize treatment based on response: one only investigated the correlation between PET parameters post-IC1 and endoscopic response after IC prior to definitive treatment (*22*); the other two had large variations in both the scanning timeline (anytime 2-4 weeks post-IC1) and the definitive therapy (surgery, chemoradiotherapy or hyperfractionated radiotherapy) (*21,23*). The strength of our study lies in the homogeneous data; the scans were carried out at 2 weeks post-IC1 and the parameters correlated specifically with outcomes following chemoradiotherapy.

We have shown that there are clear signals from $^{18}$F-FDG-PET/CT irrespective of the methodologies chosen to generate MTV. Nevertheless, if investigators choose to use the relative threshold method, TLG should be the parameter of choice as it accounts for the variable metabolic significance of individual ROIs as demonstrated by the improved predictive value of $TLG_{40\%}$ over $MTV_{40\%}$.

In contrast, we did not find pre-treatment ADC to be predictive of treatment outcome. A possible explanation for this is that a comparatively larger variation in pre-treatment ADC, notably in the PT (range 0.9-1.54 $x10^{-3}$ $mm^2/s$), was observed amongst

the responders. This appears to be driven by the high prevalence of HPV-positive disease in our patients' cohort (Fig. 6). HPV-positive oropharyngeal cancer (tonsillar and base of tongue) are known to exhibit unique histological features such as indistinct cell borders and comedo necrosis, unlike other subsites or HPV-negative disease (*24,25*). The presence of micronecrosis (not readily distinguishable on imaging) may have contributed to the unexpectedly high pre-treatment ADC values in some HPV-positive PTs. Importantly, this does not have the same negative biological impact on outcome as in HPV-negative tumours (*25*). Therefore, investigators should exercise caution interpreting ADC values for HPV-positive PT.

DW-MRI studies, in the context of chemoradiotherapy alone, have demonstrated an increase in ADC in responders and a lower increase or decrease 1-3 weeks into radiotherapy in non-responders (*26-28*). Whilst our DW-MRI data with IC showed similar trends, it was unable to distinguish eventual responders from non-responders. A possible explanation for this is the more pronounced impact of IC on the volumetric changes of tumour (Table 3) in comparison to chemoradiotherapy. Reorganisation of cellular structures and extracellular spaces following IC may have consequently dampened the 'peak' ADC increase measured in our responders, suggesting that DW-MRI should be acquired even earlier, within 1$^{st}$ week post-IC1. The only other study evaluating DW-MRI after completion of IC also found no significant correlation between ADC changes and short-term control (*29*).

We acknowledge the limitations of this study. A different PET/CT scanner was used for two patients, which may have influenced the reconstruction parameters. Four patients did not have measurable PT following diagnostic tonsillar biopsy or tonsillectomy. In addition, the cranio-caudal coverage of our MRI protocol (8 cm) meant that in three patients, involved LNs outside FOV were excluded from the analysis.

However, by including the largest nodal metastases, the dominant biology of the disease should have been captured.

## CONCLUSION

Our unique longitudinal data demonstrates that early assessment after IC1 using FMI is clinically appropriate. In addition, $^{18}$F-FDG-PET/CT-derived MTV or TLG, acquired after IC1 are predictive biomarkers for ultimate response to subsequent chemoradiotherapy. This enables identification of patients at risk of treatment failure at an early time-point, permitting treatment individualisation and consideration of alternative strategies such as radiotherapy dose-escalation or surgery. On the contrary, DW-MRI-derived ADC failed to provide any additional predictive value but our results highlighted the need for further understanding of the potential influence of HPV status on ADC measurement. This study continues to recruit and more data will become available.

## ACKNOWLEDGEMENTS

This work was undertaken in The Royal Marsden NHS Foundation Trust who received a proportion of its funding from the NHS Executive; the views expressed in this publication are those of the authors and not necessarily those of the NHS Executive. This work was supported by Cancer Research UK Head and Neck programme grant number C7224/A13407. We acknowledge the support of the National Institute for Health Research, Royal Marsden and Institute of Cancer Research Clinical Research Facility in Imaging and the Biomedical Research Centre. We also thank the radiographers, nuclear medicine technicians and research nurses (Tara Hurley, Lorna Grove, Motoko Ryugenji and Ana Santos) for their support.

## REFERENCES


1. Ghi MG, Paccagnella A, Ferrari D, et al. Concomitant chemoradiation (CRT) or cetuximab/RT (CET/RT) versus induction Docetaxel/Cisplatin/5-Fluorouracil (TPF) followed by CRT or CET/RT in patients with Locally Advanced Squamous Cell Carcinoma of Head and Neck (LASCCHN). A randomized phase III factorial study (NCT01086826). *J Clin Oncol.* 2014; 32(suppl 15):6004.
2. Hitt R, Grau JJ, Lopez-Pousa A, et al. A randomized phase III trial comparing induction chemotherapy followed by chemoradiotherapy versus chemoradiotherapy alone as treatment of unresectable head and neck cancer. *Ann Oncol*. 2013;25(1):216–225.
3. Haddad R, O'Neill A, Rabinowits G, et al. Induction chemotherapy followed by concurrent chemoradiotherapy (sequential chemoradiotherapy) versus concurrent chemoradiotherapy alone in locally advanced head and neck cancer (PARADIGM): a randomised phase 3 trial. *Lancet Oncol.* 2013;14(3):257-264.
4. Cohen EEW, Karrison TG, Kocherginsky M, et al. Phase III Randomized Trial of Induction Chemotherapy in Patients With N2 or N3 Locally Advanced Head and Neck Cancer. *J Clin Oncol.* 2014;32(25):2735-2743.
5. Machtay M, Rosenthal DI, Hershock D, et al. Organ preservation therapy using induction plus concurrent chemoradiation for advanced resectable oropharyngeal carcinoma: a University of Pennsylvania Phase II Trial. *J Clin Oncol.* 2002;20(19):3964-3971.

6. Pignon JP, le Maître A, Maillard E, Bourhis J. Meta-analysis of chemotherapy in head and neck cancer (MACH-NC): An update on 93 randomised trials and 17,346 patients. *Radiother Oncol.* 2009;92(1):4-14.

7. Wolf GT, Hong WK, Gross Fisher S, et al. Induction chemotherapy plus radiation compared with surgery plus radiation in patients with advanced laryngeal cancer. The Department of Veterans Affairs Laryngeal Cancer Study Group. *N Engl J Med*. 1991;324(24):1685-1690.

8. Ensley JF, Jacobs JR, Weaver A, et al. Correlation between response to cisplatinum-combination chemotherapy and subsequent radiotherapy in previously untreated patients with advanced squamous cell cancers of the head and neck. *Cancer*. 1984;54(5):811-814.

9. Masterson L, Moualed D, Liu ZW, et al. De-escalation treatment protocols for human papillomavirus-associated oropharyngeal squamous cell carcinoma: A systematic review and meta-analysis of current clinical trials. *Eur J Cancer*. 2014;50(15):2636-2648.

10. Lefebvre JL, Pointreau Y, Rolland F, et al. Induction chemotherapy followed by either chemoradiotherapy or bioradiotherapy for larynx preservation: the TREMPLIN randomized phase II study. *J Clin Oncol*. 2013;31(7):853-859.

11. Quon H, Brizel DM. Predictive and Prognostic Role of Functional Imaging of Head and Neck Squamous Cell Carcinomas. *Semin Radiat Oncol*. 2012;22(3):220-232.

12. Kikuchi M, Shinohara S, Nakamoto Y, et al. Sequential FDG-PET/CT after Neoadjuvant Chemotherapy is a Predictor of Histopathologic Response in Patients with Head and Neck Squamous Cell Carcinoma. *Mol Imaging Biol*. 2011;13(2):368-377.

13. Kim S, Loevner L, Quon H, et al. Diffusion-Weighted Magnetic Resonance Imaging for Predicting and Detecting Early Response to Chemoradiation Therapy of Squamous Cell Carcinomas of the Head and Neck. *Clin Cancer Res*. 2009;15(3):986-994.

14. Kato H, Kanematsu M, Tanaka O, et al. Head and neck squamous cell carcinoma: usefulness of diffusion-weighted MR imaging in the prediction of a neoadjuvant therapeutic effect. *Eur Radiol.* 2009;19(1):103-109.

15. Allal AS, Slosman DO, Kebdani T, Allaoua M, Lehmann W, Dulguerov P. Prediction of outcome in head-and-neck cancer patients using the standardized uptake value of 2-[18F]fluoro-2-deoxy-D-glucose. *Int J Radiat Oncol Biol Phys*. 2004;59(5):1295-1300.

16. Schwartz DL, Rajendran J, Yueh B, et al. FDG-PET prediction of head and neck squamous cell cancer outcomes. *Arch Otolaryngol Head Neck Surg*. 2004;130(12):1361-1367.

17. Han M, Kim SY, Lee SJ, Choi JW. The Correlations Between MRI Perfusion, Diffusion Parameters, and 18F-FDG PET Metabolic Parameters in Primary Head-and-Neck Cancer: A Cross-Sectional Analysis in Single Institute. *Medicine (Baltimore).* 2015;94(47):e2141.

18. Welsh L, Panek R, McQuaid D, et al. Prospective, longitudinal, multi-modal functional imaging for radical chemo-IMRT treatment of locally advanced head and neck cancer: the INSIGHT study. *Radiat Oncol.* 2015;10(1):112.

19. Larson SM, Erdi Y, Akhurst T, et al. Tumor Treatment Response Based on Visual and Quantitative Changes in Global Tumor Glycolysis Using PET-FDG Imaging. The Visual Response Score and the Change in Total Lesion Glycolysis. *Clin Positron Imaging*. 1999;2(3):159-171.

20. Pak K, Cheon GJ, Nam HY, et al. Prognostic Value of Metabolic Tumor Volume and Total Lesion Glycolysis in Head and Neck Cancer: A Systematic Review and Meta-Analysis. *J Nucl Med.* 2014;55(6):884-890.

21. Semrau S, Haderlein M, Schmidt D, et al. Single-cycle induction chemotherapy followed by chemoradiotherapy or surgery in patients with head and neck cancer: What are the best predictors of remission and prognosis? *Cancer*. 2014;121(8):1214-1222.

22. Gavid M, Prevot-Bitot N, Timoschenko A, Gallet P, Martin C, Prades JM. [18F]-FDG PET-CT prediction of response to induction chemotherapy in head and neck squamous cell carcinoma: Preliminary findings. *Eur Ann Otorhinolaryngol Head Neck Dis.* 2015;132(1):3-7.

23. Kikuchi M, Nakamoto Y, Shinohara S, et al. Early evaluation of neoadjuvant chemotherapy response using FDG-PET/CT predicts survival prognosis in patients with head and neck squamous cell carcinoma. *Int J Clin Oncol*. 2012;18(3):402-410.

24. El-Mofty SK, Lu DW. Prevalence of Human Papillomavirus Type 16 DNA in Squamous Cell Carcinoma of the Palatine Tonsil, and Not the Oral Cavity, in Young Patients: A Distinct Clinicopathologic and Molecular Disease Entity. *Am J Surg Pathol.* 2003;27(11):1463-70.

25. Chernock RD, El-Mofty SK, Thorstad WL, Parvin CA, Lewis JS. HPV-Related Nonkeratinizing Squamous Cell Carcinoma of the Oropharynx: Utility of Microscopic Features in Predicting Patient Outcome. *Head Neck Pathol.* 2009;3(3):186-194.

26. Kim S, Loevner L, Quon H, et al. Diffusion-weighted magnetic resonance imaging for predicting and detecting early response to chemoradiation

therapy of squamous cell carcinomas of the head and neck. *Clin Cancer Res.* 2009;15(3):986-94.

27. Vandecaveye V, Dirix P, De Keyzer F, et al. Predictive value of diffusion-weighted magnetic resonance imaging during chemoradiotherapy for head and neck squamous cell carcinoma. *Eur Radiol.* 2010;20(7):1703-1714.

28. Matoba M, Tuji H, Shimode Y, et al. Fractional change in apparent diffusion coefficient as an imaging biomarker for predicting treatment response in head and neck cancer treated with chemoradiotherapy. *AJNR Am J Neuroradiol.* 2014;35(2):379-385.

29. Berrak S, Chawla S, Kim S, et al. Diffusion weighted imaging in predicting progression free survival in patients with squamous cell carcinomas of the head and neck treated with induction chemotherapy. *Acad Radiol.* 2011;18(10):1225-1232.

## FIGURE LEGENDS

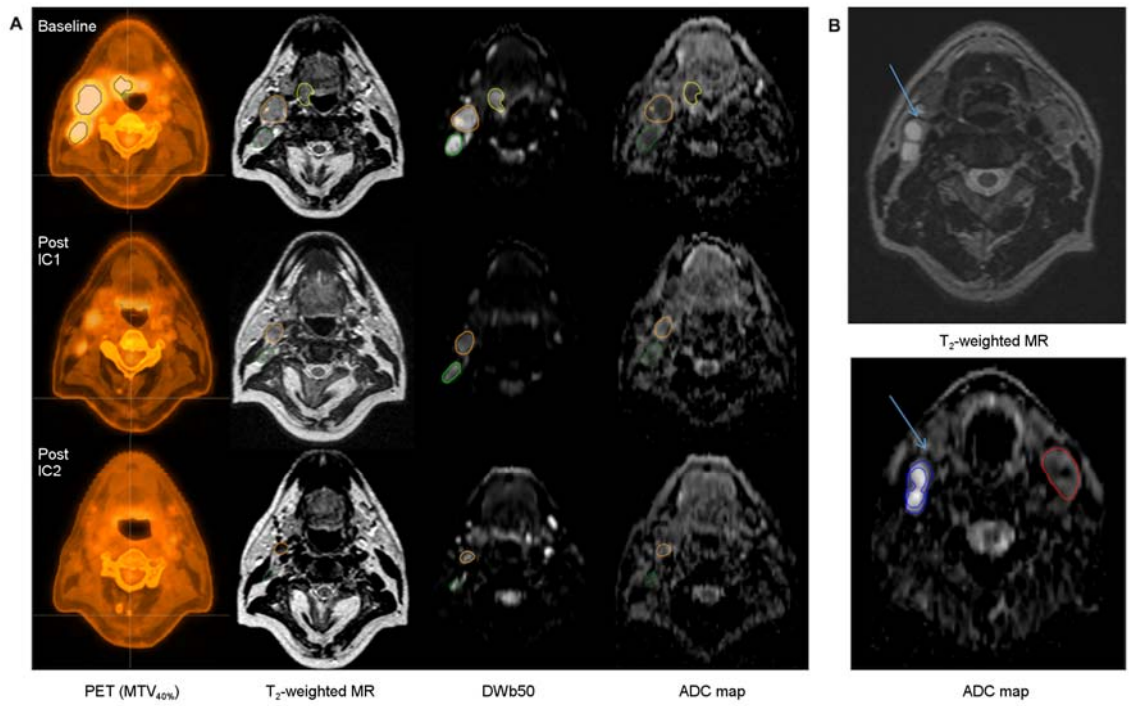


**FIGURE 1**. **A**: A panel of serial PET/CT, $T_2$-weighted, b50 and, ADC images (from left to right) alongside respective ROIs contours in a patient with T2N2bM0 HPV-positive oropharyngeal SCC; and **B**: An example of ROI definition on ADC maps with reference to anatomical image ($T_2$-weighted). The arrows highlight active exclusion of necrotic/cystic regions in the right level II LNs.

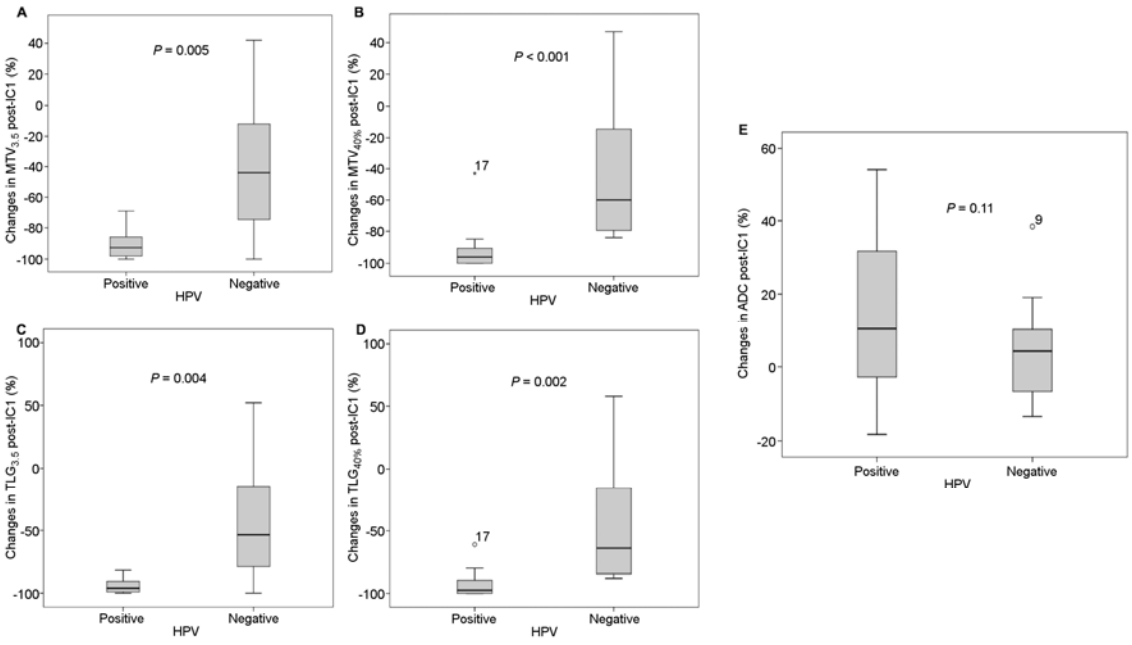


**FIGURE 2**. Boxplots of changes post-IC1, grouped by HPV status, for **A**-$MTV_{3.5}$, **B**-$MTV_{40\%}$, **C**-$TLG_{3.5}$, **D**-$TLG_{40\%}$ and **E**-Cumulative ADC (PT and LNs).

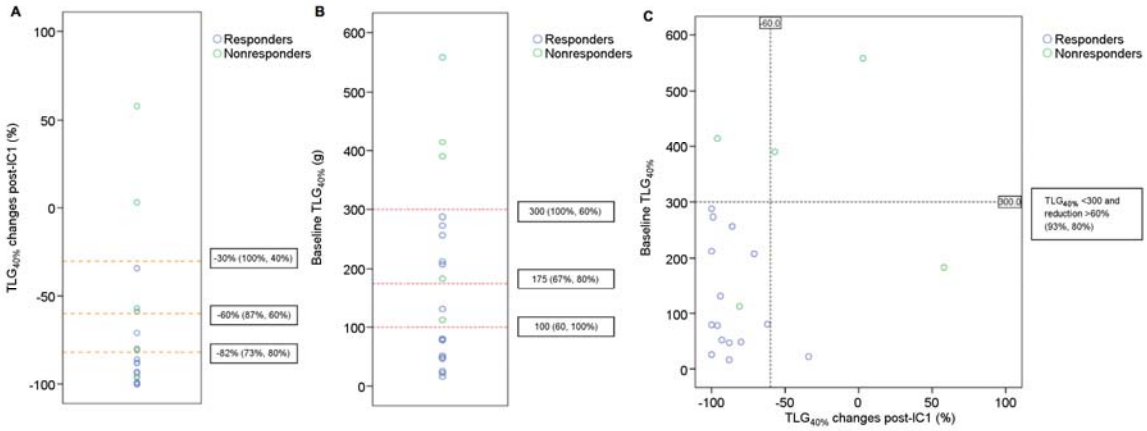


**FIGURE 3. A**: A dot-plot of $\Delta TLG_{40\%}$ post-IC1 with suggested ROC co-ordinates (-30%, -60% and -82%) as cut-offs for predicting complete response to chemoradiotherapy. The optimal sensitivity and specificity achieved by $\Delta TLG_{40\%}$ post-IC1 as a standalone parameter was 73% and 80% respectively (-60%); **B**: A dot-plot of baseline $TLG_{40\%}$ with suggested ROC co-ordinates (100g, 175g and 300 grams) as cut-offs. The cut-offs of 100 g (60%,100%) was considered optimal; and **C**: A scatter plot of baseline $TLG_{40\%}$ (Y-axis) against $\Delta TLG_{40\%}$ post-IC1 (X-axis). Iteratively, a combination of baseline $TLG_{40\%}$ <300 g and $TLG_{40\%}$ post-IC1 reduction >60% gives an improved balance of sensitivity and specificity (93% and 80%) i.e. not over- or underestimating non-responders.

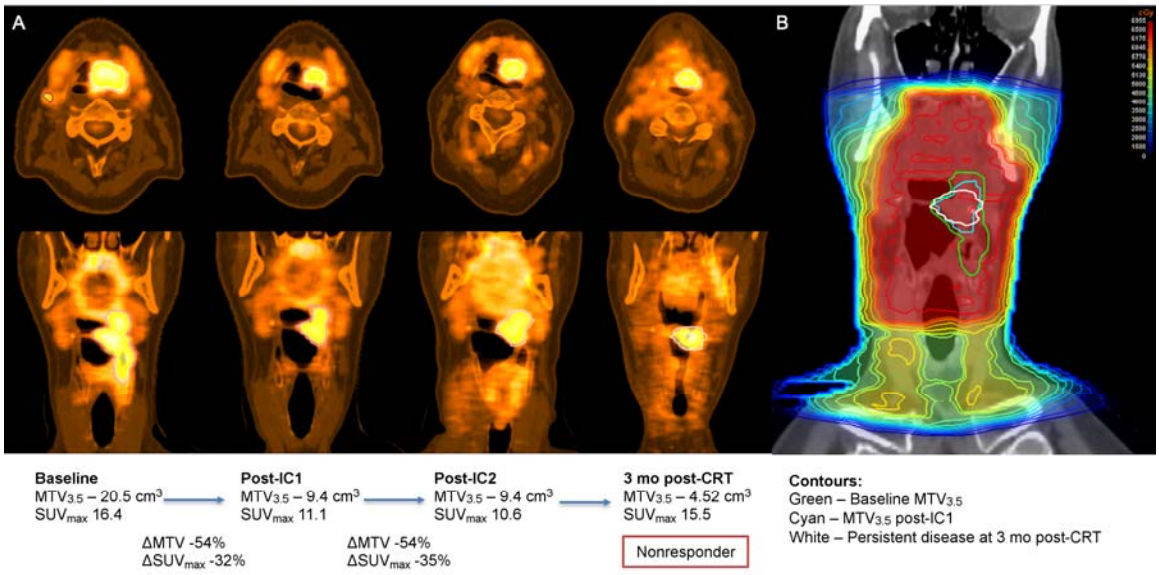


**FIGURE 4**. **A:** Serial $^{18}$F-FDG-PET/CT in a non-responder with T3N2bM0 oropharyngeal SCC. Following initial response, no further significant reduction in $MTV_{3.5}$ and SUVmax was observed between IC1 and IC2. This would be considered a suboptimal response ($MTV_{3.5}$ reduction <55%) with higher risk of subsequent chemoradiotherapy failure; and **B:** Coronal view of radiotherapy planning CT and dosimetry from clinical plan showing in-field failure. There was a 86% volume overlap between persistent disease post-chemoradiotherapy with $MTV_{3.5}$ post-IC1.

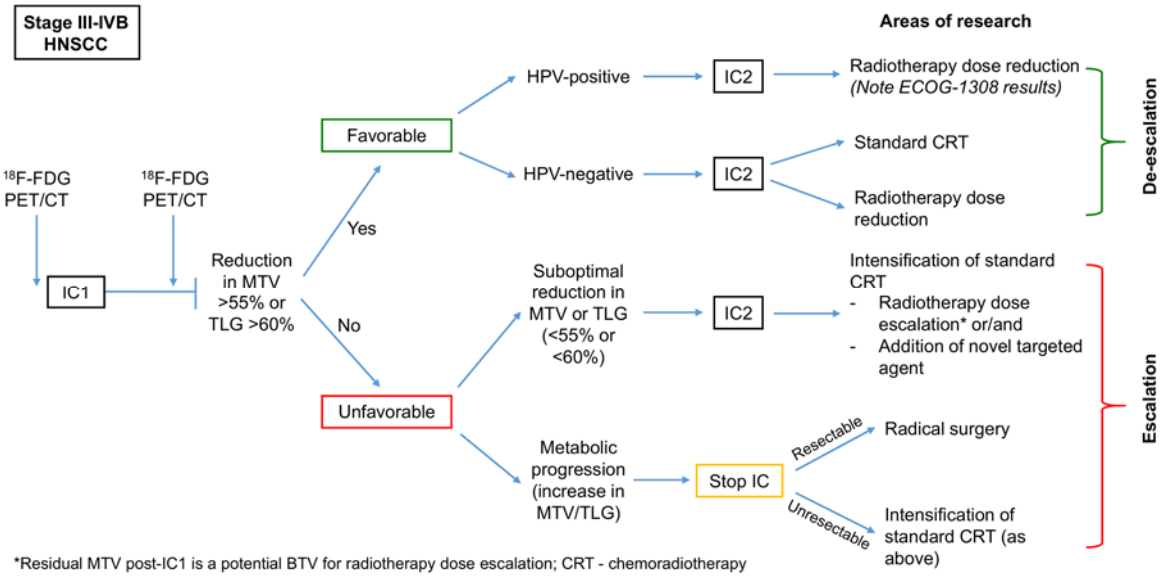


**FIGURE 5.** A flowchart illustrating how stratification of patients during IC using FMI (based on response) could guide subsequent treatment personalization. Escalation or de-escalation of radical chemoradiotherapy are now a topical area of research.

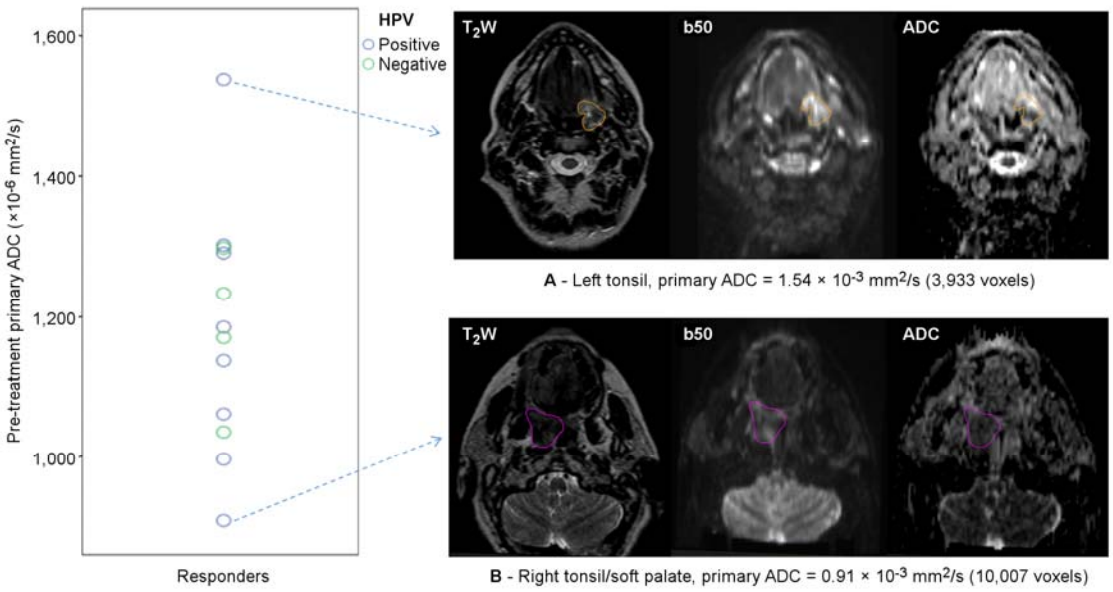


**FIGURE 6**. A dot-plot showing the distribution of pre-treatment ADC for PT in responders, categorised by HPV status with representative DW images for cases with the highest (**A**) and lowest (**B**) values. It was evident that HPV-positive PTs were accountable for the large variation of ADC values in this group.

**TABLE 1. Summary of patient and tumour characteristics**

| | |
|---|---|
| Number of patients | 20 |
| Age (years), median (range) | 63, (47 - 69) |
| Sex (%) | |
| Female | 2 (10) |
| Male | 18 (80) |
| Primary location (%) | |
| Oropharynx | 18 (80) |
| Hypopharynx/larynx | 2 (20) |
| HPV status (%) | |
| Positive | 12 (60) |
| Negative | 8 (40) |
| Grade (%) | |
| G1-2 | 7 (35) |
| G3 | 13 (65) |
| Stage (%) | |
| T | |
| 1-2 | 11 (55) |
| 3-4 | 9 (45) |
| N | |
| 0-1 | 2 (10) |
| 2-3 | 18 (90) |
| Induction chemotherapy (%) | |
| Cisplatin/5-fluorouracil | 4 (20) |
| Carboplatin/5-fluorouracil | 5 (25) |
| TPF | 11 (55) |
| Concomitant chemotherapy (%) | |
| Cisplatin | 8 (40) |
| Carboplatin | 8 (40) |
| Cis/Carbo* | 3 (15) |
| None | 1 (5) |

* Cisplatin on Day 1 switched to Carboplatin on Day 29

**TABLE 2. Comparison of FMI parameters between responders and non-responders**

| FMI parameters | Responders (n=15) | Non-responders (n=5) | p value† | ROC (AUC) |
|---|---|---|---|---|
| **$MTV_{40\%}$ ($cm^3$)** | | | | |
| Baseline | 15.9±14.0 | 33.0±14.9 | 0.040* | 0.813 |
| Δ post-IC1 | -84.4±20.5% | -34.4±59.7% | 0.086 | - |
| **$MTV_{3.5}$ ($cm^3$)** | | | | |
| Baseline | 21.9±16.4 | 56.9±24.7 | 0.011* | 0.880 |
| Δ post-IC1 | -84.3±19.4% | -29.6±55.9% | 0.033* | 0.820 |
| **$TLG_{40\%}$ (g)** | | | | |
| Baseline | 121.2±98.7 | 359.4±201.8 | 0.021* | 0.853 |
| Δ post-IC1 | -85.9±18.6% | -34.6±64.1% | 0.042* | 0.807 |
| **$TLG_{3.5}$ (g)** | | | | |
| Baseline | 156.4±139.6 | 481.0±254.1 | 0.013* | 0.880 |
| Δ post-IC1 | -87.4±18.1% | -32.1±60.4% | 0.042* | 0.807 |
| **SUVmax (g/ml)** | | | | |
| Baseline | 14.1±6.5 | 17.8±3.0 | 0.150 | - |
| Δ post-IC1 | -47.0±27.2% | -23.8±34.0% | 0.119 | - |
| **SUVmean (g/ml)** | | | | |
| Baseline | 7.9±3.9 | 10.4±2.2 | 0.142 | - |
| Δ post-IC1 | -34.3±31.7% | -26.8±42.8% | 0.230 | - |
| **ADC primary ($x10^{-3}$ $mm^2/s$)** | | | | |
| Baseline (16 ROIs) | 1.18±0.17 | 1.07±0.10 | 0.262 | - |
| Post-IC1 (12 ROIs) | 1.23±0.17 | 1.08±0.13 | 0.089 | - |
| Δ post-IC1 | 9.2±21.9% | 2.2±9.4% | 1.000 | - |
| **ADC LNs ($x10^{-3}$ $mm^2/s$)** | | | | |
| Baseline (30 ROIs) | 0.99±0.14 | 1.05±0.18 | 0.437 | - |
| Post-IC1 (29 ROIs) | 1.13±0.18 | 1.02±0.24 | 0.384 | - |
| Δ post-IC1 | 14.7±18.9% | 0.6±8.4% | 0.159 | - |

Results reported as mean±standard deviation; Δ post-IC1 = (Post-IC1-baseline)/baseline x 100%; † Comparison between responders and non-responders; *Significant

**TABLE 3. Longitudinal FDG-PET and MRI parameters (n=17)**

| FMI parameters | Baseline | Δ post-IC1 | Δ post-IC2 | p value† |
|---|---|---|---|---|
| **$MTV_{40\%}$ ($cm^3$)** | | | | |
| Combined | 21.6±16.4 | -70.9±41.5% | -76.4±47.1% | 0.102 |
| **$MTV_{3.5}$ ($cm^3$)** | | | | |
| Combined | 33.3±24.8 | -66.2±40.8% | -71.6±45.0% | 0.362 |
| **$TLG_{40\%}$ (g)** | | | | |
| Combined | 198.7±171.4 | -71.3±43.2% | -75.1±53.2% | 0.195 |
| **$TLG_{3.5}$ (g)** | | | | |
| Combined | 261.3±230.7 | -69.6±42.4% | 73.0±50.5% | 0.363 |
| **SUVmax (g/ml)** | | | | |
| Combined | 15.0±6.3 | -37.1±30.5% | -46.9±31.0% | 0.065 |
| **SUVmean (g/ml)** | | | | |
| Combined | 8.5±3.8 | -23.8±23.1% | -30.8±25.8% | 0.071 |
| **MR volume ($cm^3$)** | | | | |
| Combined | 24.7±18.7 | -50.7±31.2% | -60.6±38.1% | 0.006* |
| Primary | 13.6±16.5 | -68.0±29.6% | -77.8±28.2% | 0.019* |
| LNs | 14.4±12.8 | -36.8±35.1% | -48.4±43.4% | 0.020* |
| **ADC ($x10^{-3}$ $mm^2/s$)** | | | | |
| Primary | 1.15±0.16 | 11.7±20.2% | 18.5±9.9% | 0.137 |
| LNs | 1.00±0.15 | 10.8±16.9% | 12.4±24.2% | 0.619 |

Results reported as mean±standard deviation; Δ post IC1 = (Post-IC1-baseline)/baseline x 100%; Δ post IC2 = (Post-IC2 - baseline)/baseline x 100%;

† Paired comparison between Δ post-IC1 and Δ post-IC2; *Significant